ORNL-5410

LOCKHEED MARTIN ENERGY RESEARCH LIBRARIES

3 4456 0515141 1

Formation of Iron Carbonyl Between a 1/2% Mo Steel and High-Pressure Gases Containing Carbon Monoxide

H. Inouye
J. H. DeVan

OAK RIDGE NATIONAL LABORATORY
CENTRAL RESEARCH LIBRARY
CIRCULATION SECTION
4500N ROOM 175
LIBRARY LOAN COPY
DO NOT TRANSFER TO ANOTHER PERSON
If you wish someone else to see this report, send in name with report and the library will arrange a loan.
UCN 7969 3 9-77

OAK RIDGE NATIONAL LABORATORY
OPERATED BY UNION CARBIDE CORPORATION · FOR THE DEPARTMENT OF ENERGY

Printed in the United States of America. Available from
National Technical Information Service
U.S. Department of Commerce
5285 Port Royal Road, Springfield, Virginia 22161
Price: Printed Copy $4.50; Microfiche $3.00

This report was prepared as an account of work sponsored by an agency of the United States Government. Neither the United States Government nor any agency thereof, nor any of their employees, contractors, subcontractors, or their employees, makes any warranty, express or implied, nor assumes any legal liability or responsibility for any third party's use or the results of such use of any information, apparatus, product or process disclosed in this report, nor represents that its use by such third party would not infringe privately owned rights.

LOCKHEED MARTIN ENERGY RESEARCH LIBRARIES

3 4456 0515141 1

ORNL-5410
Distribution
Category UC-90d

Contract No. W-7405-eng-26

METALS AND CERAMICS DIVISION

FORMATION OF IRON CARBONYL BETWEEN A 1/2% Mo STEEL AND HIGH-PRESSURE GASES CONTAINING CARBON MONOXIDE

H. Inouye and J. H. DeVan

Date Published - May, 1978

OAK RIDGE NATIONAL LABORATORY
Oak Ridge, Tennessee 37830
operated by
UNION CARBIDE CORPORATION
for the
DEPARTMENT OF ENERGY

CONTENTS

ABSTRACT 1
INTRODUCTION 1
PREVIEW WORK 2
EXPERIMENTAL PROCEDURE 3
Autoclave System 3
Test Procedure 5
Calibration of the AAS 5
RESULTS 6
Flow Rate Effects 6
Temperature Effects 10
Pressure Effects 11
Effect of Test Gases on 1/2% Mo Steel 11
Carbonyl Formation from Type 316 Stainless Steel 13
DISCUSSION 13
SUMMARY AND CONCLUSIONS 18
ACKNOWLEDGMENTS 19
REFERENCES 19

FORMATION OF IRON CARBONYL BETWEEN A 1/2% Mo STEEL AND HIGH-PRESSURE GASES CONTAINING CARBON MONOXIDE

H. Inouye and J. H. DeVan

ABSTRACT

An atomic absorption spectrophotometer was used to measure the formation of iron carbonyl between 1/2% Mo steel pipes and flowing high-pressure gases (to 6.9 MPa) containing carbon monoxide. The net formation rate, $\dot{r}$, of iron carbonyl was measured as a function of the velocity, temperature, and pressure of the gases to determine the conditions that prevent its formation. These variables and the gas composition affected $\dot{r}$ as follows: (1) Rate $\dot{r}$ increases linearly with the gas velocity. Under equilibrium conditions, $\dot{r}$ is proportional to the gas velocity, but it reaches a limiting value above a critical gas velocity when equilibrium is not maintained. (2) Between 44 and 266°C, $\dot{r}$ increases with temperature to a sharp maximum at 177°C in a gas mixture containing 17 CO—51 H_2—30 CH_4—2 CO_2 (vol %). The corresponding maximum in carbon monoxide occurs at 245°C. The data predict that iron carbonyl formation will be negligible above 270°C in the gas mixture or above 285°C in carbon monoxide. (3) Rate $\dot{r}$ depends on P_{CO} in accordance with the equation $\dot{r} = kP_{CO}^{n}$, where n = 4 to 5 under equilibrium conditions and n = 2 off equilibrium. The analytical procedure used to detect ±6 vpb (volume parts per billion) of iron carbonyl and ±1.5 vpb of nickel carbonyl in flowing high pressure gases is described. The reaction rates are described in terms of kinetics and thermodynamic equilibrium.

INTRODUCTION

The production of synthetic natural gas (SNG) from coal involves reacting hydrogen and carbon monoxide over a Raney nickel catalyst to produce methane. Deposition of iron on the methanation catalyst converts it to a Fisher-Tropsch catalyst, and this is thought to be one of the reasons for the decrease in the methane yield during the lifetime of the catalyst.[1] Iron pentacarbonyl formed by the reaction of carbon monoxide with the steel piping leading to the methanation reactor is

believed to be the source of the iron.[2] Therefore, this study was directed toward finding practical methods of preventing carbonyl formation in structural steels, initially through a systematic evaluation of various steels, then by a study of preventive techniques such as coatings. This report summarizes the variables governing the formation of iron carbonyl resulting from the reaction of 1/2% Mo steel (A 334-P1) with a flowing gas mixture containing 17 CO—51 H_2—30 CH_4—2 CO_2 and with 100 CO (vol %) between 44 and 266°C and gas pressures to 6.98 MPa (1000 psi). Iron and nickel carbonyl formation between type 316 stainless steel and the above gases was also briefly investigated.

PREVIEW WORK

A literature survey[3] of the thermodynamic and kinetic data for iron and nickel carbonyl formation was completed before we started this study. The principal conclusions of this survey are summarized below. At moderate temperatures (100—250°C) and pressures (0.1—101 MPa) the attack upon steel pipes by carbon monoxide is limited by the reaction rate. In static carbon monoxide the formation rate, $\dot{r}$, of iron carbonyl from iron powder[4] or millings[5] reached a maximum at 200°C for carbon monoxide pressures between 10 and 100 MPa. An analysis of data from Ref. 5 showed that $\dot{r}$ increased significantly with the gas velocity; however, the effect of temperature on carbonyl formation in flowing gases was not determined.

Stoffel[6] determined that $\dot{r}$ depended on $P_{CO}^{2.0}$, whereas the data of Mond and Wallis[4] gave a pressure dependence of $P_{CO}^{1.67}$. A pair of data points in Ref. 5 indicate that $\dot{r}$ depends on $P_{CO}^{1.76}$. Table 1 (based on Ref. 5) is a summary of the corrosion of steels of interest in carbon monoxide and in a gas mixture containing 30 CO—60 H_2—10 N_2 (vol %) at 101 MPa (1000 atm). Although a direct comparison of the data in each test gas cannot be made (because the dependence of $\dot{r}$ on P_{CO} in the gas mixture is unknown), the data show increasing resistance to carbon monoxide attack as the chromium and nickel contents in the steel increase. In contrast, an increase in the carbon content of iron from 0.1 to 2.9% (cast iron) increases the corrosion rate by a factor

Table 1. Effect of Alloy Composition on the Corrosion of Steels Exposed to Gases Containing Carbon Monoxide[a]

Steel Composition (wt %)	Weight Change, %, in	
	Carbon Monoxide	30 CO–60 H_2–10 N_2
0.1 C	−1.98	*b*
2.9 C (cast iron)	−71.58	*b*
1/2 Mo–0.15 C	−0.87	−2.91
3 1/4 Cr–1/2 Mo	−0.18	−0.04
5 1/4 Cr–2 1/4 Si–1/2 Mo	−0.07	−0.04
14.2 Cr	0.00	0.00
18 Cr–8 Ni	+0.01	+0.01
5 Ni	−0.38	−0.03
23 Ni	−0.02	0.00

[a]Rods 0.6 mm diam × 40 mm long exposed for 402 hr at 200°C to static gases, at 101 MPa (1000 atm) pressure. Adapted from H Pichler and H. Wallenda, *Brennst. Chem.* 21: 133 (1940).

[b]Not tested.

of 35! The cast iron rod was reduced to a skeleton of "phosphide eutectic of cast iron with a narrow residue of ferrite" having the same initial dimensions. In the case of all steels, any measurable amount of corrosion by carbon monoxide was accompanied by a net increase in the carbon content due to the deposition of free carbon on the surface. Data from Ref. 5 further show that the corrosion rate of the 1/2% Mo–0.15% C steel can be expected to be significantly greater in the CO-H_2-N_2 mixture than in carbon monoxide (see Table 1).

EXPERIMENTAL PROCEDURE

Autoclave System

Figure 1 is the schematic arrangement of the type 316 stainless steel system used to measure the formation rate of iron carbonyl. The two autoclaves placed in series are each 159 mm OD by 16 mm wall by

ORNL-DWG 77-20779

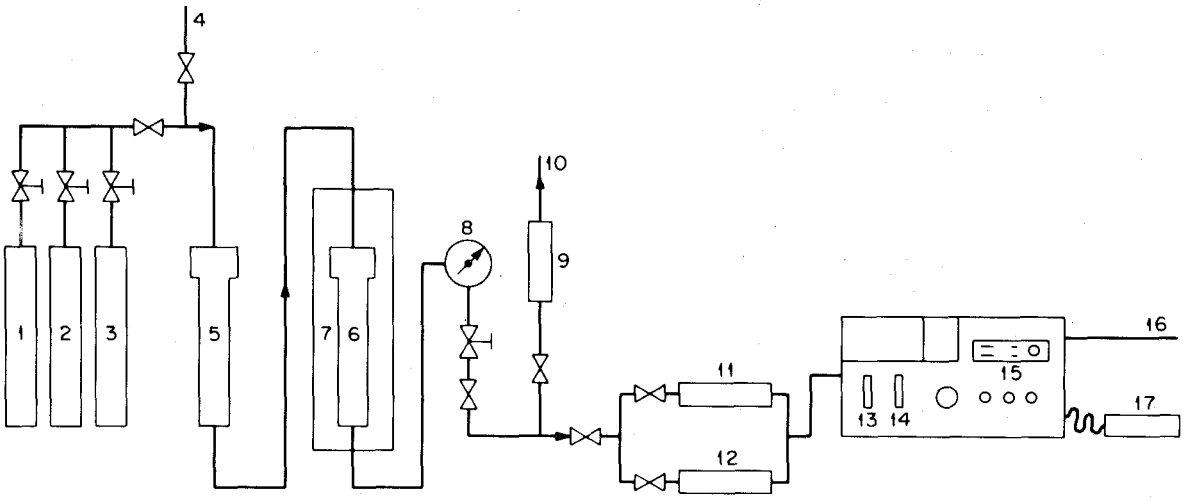

1. MIXED GAS TANK
2. CARBON MONOXIDE TANK
3. HYDROGEN TANK
4. HIGH PRESSURE VENT
5. ACTIVATED CHARCOAL AUTOCLAVE
6. SPECIMEN AUTOCLAVE
7. FURNACE
8. HEISE PRESSURE GAGE
9. FLOWMETER
10. LOW PRESSURE VENT
11. FIBERFRAX FILTER
12. ACTIVATED CHARCOAL FILTER
13. FUEL FLOWMETER
14. AIR FLOWMETER
15. ATOMIC ABSORPTION SPECTROPHOTOMETER
16. AIR SUPPLY LINE
17. CHART RECORDER

Fig. 1. The Autoclave System and the Atomic Absorption Spectrophotometer Arranged as Shown was Used to Measure ±6 vpb and ±1.2 vpb of Iron and Nickel Carbonyls, Respectively, in Flowing Gases to 6.9 MPa (1000 psi).

705 mm long. The test gas from gas cylinders flows continuously through a bed of activated charcoal at room temperature in the first autoclave to remove any metal carbonyls that might be present. Steel specimens are heated to the reaction temperature in the second autoclave and are then allowed to react with the gas leaving the charcoal trap. The effluent gas from the reaction vessel is cooled and depressurized to normal temperature and pressure (20°C and 0.1 MPa) and analyzed for its carbonyl content with an atomic absorption spectrophotometer (AAS).

Pressure regulators on the gas cylinders and a Heise high-precision absolute pressure gage were used to control gas pressures to ±69 kPa during a run. The flow rates were adjusted as desired by regulating the rate at which the effluent gases were vented to the exhaust system. The test gases were supplied in steel tanks at 10.3 MPa and were used without further treatment except as noted above. The vendors' analyses of the gas mixture, which were within 2% of the nominal, were assumed to be

correct. The gas entering the reaction vessel was preheated to within 5°C of the autoclave temperature with heater tapes around the feed lines. A three-zone furnace around the specimen autoclave was used to hold its temperature to within ±1°C along its 700-mm length.

Test Procedure

The 1/2% Mo steel specimen consisted of four lengths of pipe each 33.3 mm OD by 4.75 mm wall thickness by 600 mm long and coated on the outside with water glass (Na_2SiO_3) to exclude contact with the test gases. The specimen surface area exposed to the gases was calculated to be 1795 cm^2. Forty-eight aluminum rods, also 600 mm long, filled the bore of the pipes and the spaces between the pipes and the autoclave wall to reduce the void volume and area (2881 cm^3 and 42.43 cm^2), to increase the heat capacity of the autoclave, and to reduce the temperature gradient.

In a typical run, the steel pipes are pretreated in 1.03 MPa (150 psi) static hydrogen for at least 16 hr at 150°C or at the test temperature if over 150°C. After the system is vented and hydrogen is purged with the flowing test gas, the system is pressurized and the AAS is placed in operation. The carbonyl concentration in the effluent test gases is continuously measured until a constant value is reached for each gas flow. Experimentally, this point was reached after 1.5 complete volume changes in the autoclave gases. The net formation rate of iron carbonyl is computed as the product of the volume fraction of iron carbonyl, as determined by the AAS, and the volume flow rate of the effluent gas at normal temperature and pressure (NTP). At the conclusion of a run, the system is depressurized, and the steel pipes are reconditioned in hydrogen before the next run.

Calibration of the AAS

Brief's technique[7] with minor modifications was used to calibrate the AAS. In this technique the iron or nickel carbonyl in a 50-liter sample of a reference gas is absorbed in an appropriate solution, then

complexed to form a colored solution. The optical density of the complexed metal in the solution is measured with the AAS in terms of absorption units and compared with standard solutions containing known levels of iron or nickel. The calibrated reference gas is then used as the standard to determine the carbonyl concentration in the effluent gas from the autoclave. The uncertainty in the output of the AAS was about ±5 absorbance units, and a sensitivity of 1.3 vpb per absorbance unit for iron carbonyl gives an analytical capability of detecting ±6 vpb. For nickel carbonyl the sensitivity was 0.3 vpb per absorbance unit or a capability of detecting ±1.5 vpb.

RESULTS

Flow Rate Effects

Typically the iron carbonyl concentration in the effluent gas from the specimen autoclave decreased uniformly with the gas velocity* as shown in Fig. 2. The product of the iron carbonyl concentration (expressed as vpb) and the gas flow rate (liters/min at NTP) is the formation rate of iron carbonyl in units of nanoliters (at NTP) per minute. The specific formation rate, $\dot{r}$, is defined as the rate of iron carbonyl formation per square centimeter of reacting surface and is determined by dividing the formation rate (nl at NTP/min) by the specimen surface (1795 cm^2). For convenience, figures showing reaction rates also give the equivalent grams of iron removed per square foot per year. The specific formation rate, $\dot{r}$, increases with the gas velocity up to a critical velocity and remains constant at higher velocities (Fig. 3). The ranges of values for $\dot{r}$ above the critical velocity, V_c, for various temperatures and pressures are summarized in Table 2. On the average, V_c is 10.2 cm/min in the mixed gases and increases to 27.8 cm/min in carbon monoxide and is independent of temperature, pressure, and $\dot{r}$. In the higher temperature

*Gas velocity (cm/min) = flow rate at the test conditions (cm^3/min) ÷ 42.43 cm^2 (void cross section of autoclave).

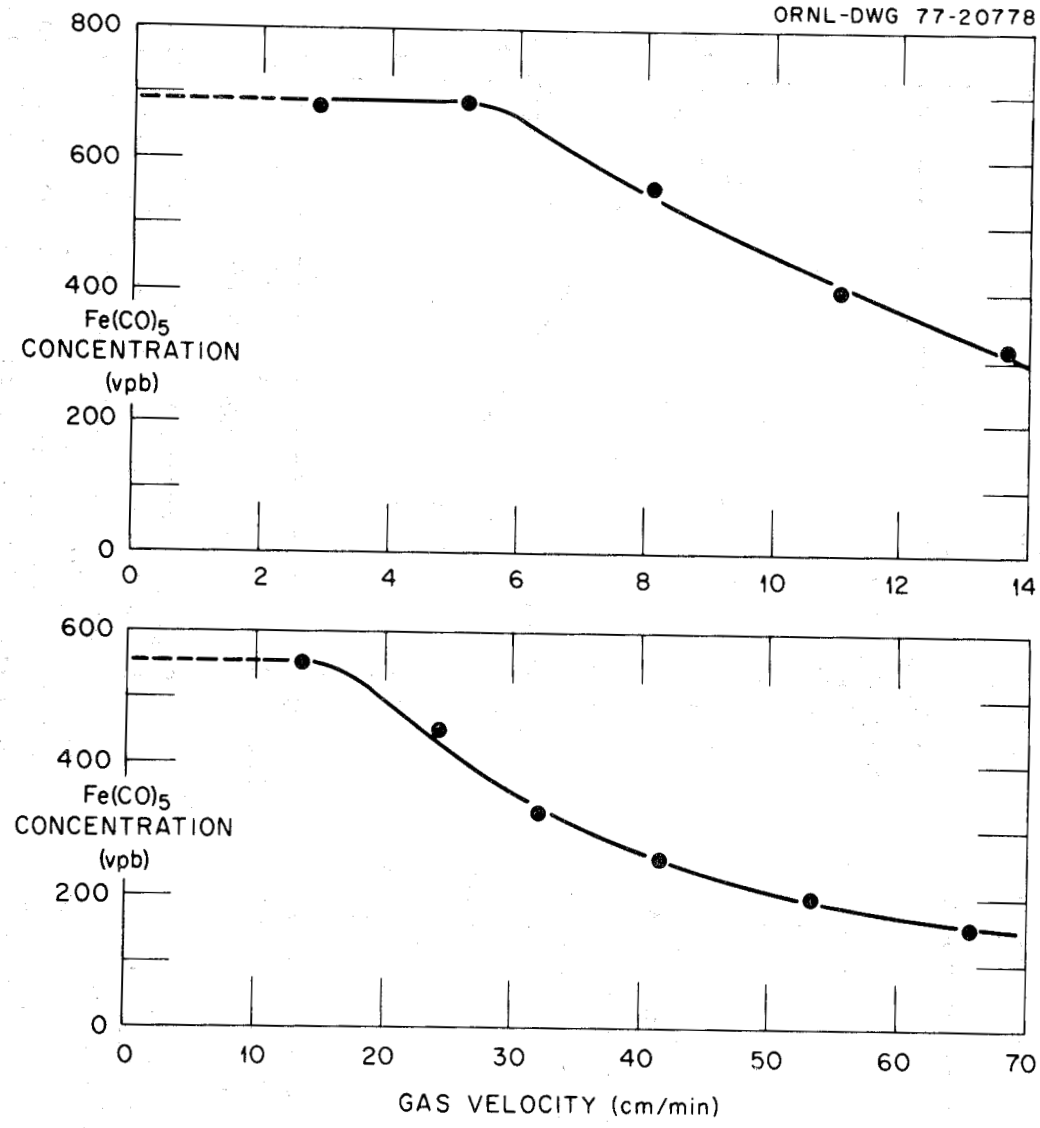

Fig. 2. Iron Carbonyl Concentration in Flowing Gases Decreases With the Gas Velocity When the Reaction is Governed by the Formation Rate. (a) In 5.5 MPa (800 psi) mixed gases at 155°C. (b) In 1.2 MPa (170 psi) carbon monoxide at 220°C.

runs the iron carbonyl concentration was independent of the gas velocity [Fig. 4(a)]. Under these conditions $\dot{r}$ is calculated to increase linearly with the gas velocity as shown in Fig. 4(b). This behavior was observed in runs 4, 20, 25, and possibly 3 and 17 in Table 2.

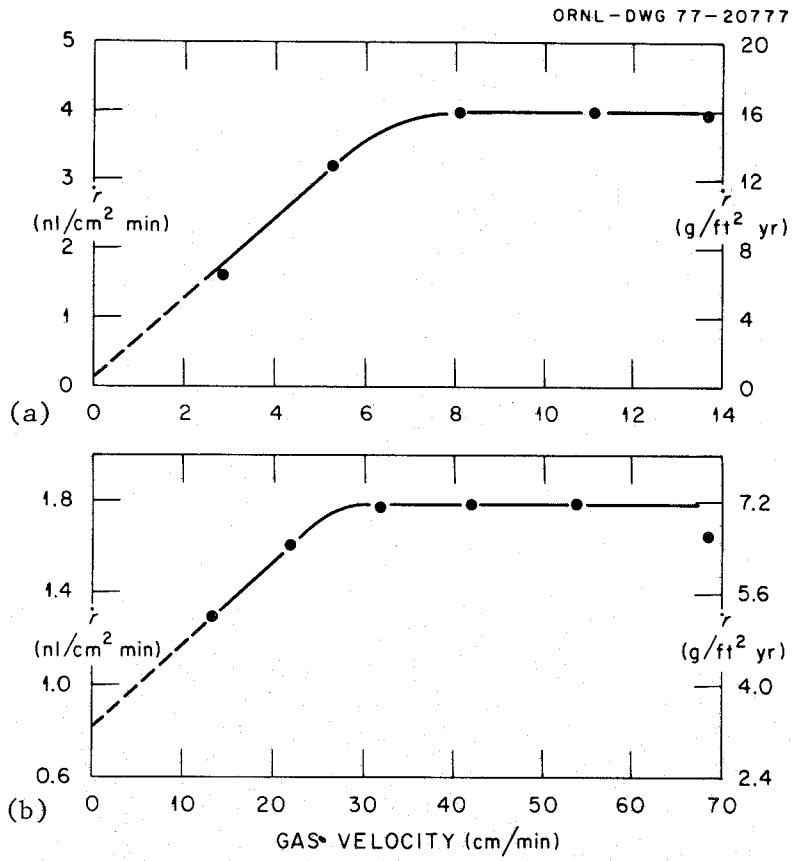

Fig. 3. The Formation Rate, $\dot{r}$, of Iron Carbonyl Increases with the Gas Velocity to a Limiting Value When the Extent of Reaction is Governed by the Formation Rate. (a) In 5.5 MPa (800 psi) mixed gases at 155°C. (b) In 1.2 MPa (170 psi) carbon monoxide at 220°C.

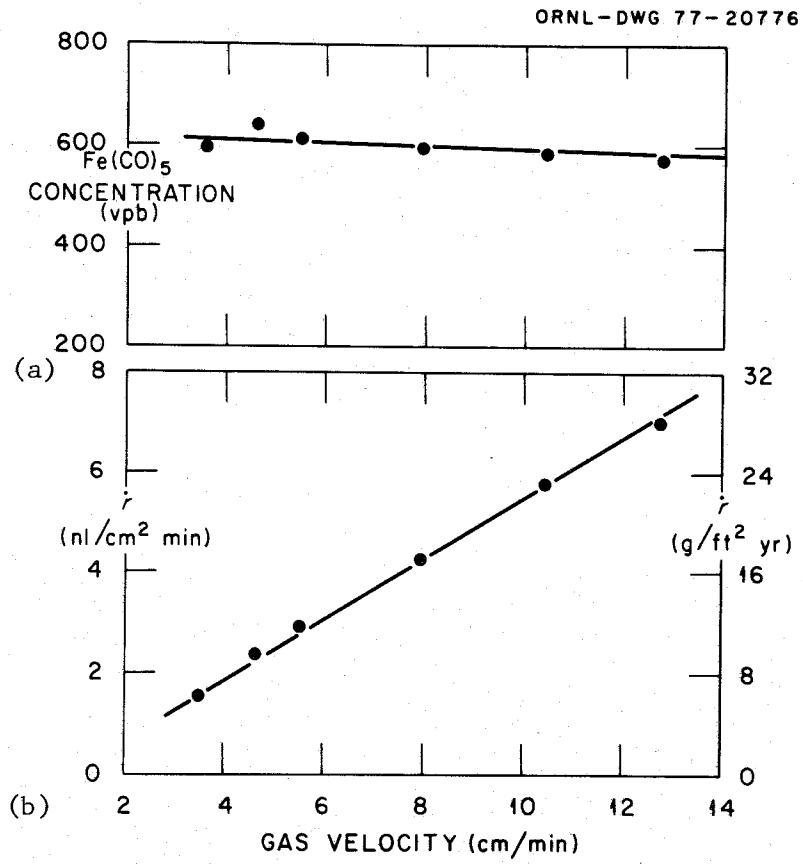

Fig. 4. Iron Carbonyl Formation When the Reaction Between the Steel and Carbon Monoxide is Governed by Equilibrium. Steel was exposed to 6.9 MPa (1000 psi) mixed gases at 177°C. (a) The concentration is independent of the gas velocity. (b) the net rate $\dot{r}$ increases linearly with gas velocity.

Table 2. Critical Velocities, V_c, for the Formation Rate, $\dot{r}$, of Iron Carbonyl Between a 1/2% Mo Steel and Gases Containing Carbon Monoxide

Run	Temperature (°C)	Pressure (MPa)	Pressure (psi)	V_c[a] (cm^2/min)	$\dot{r}$ (nl/cm^2 min)[b]
			In Mixed Gases		
3	200	6.9	1000	11[c]	5.38
4	177	6.9	1000	Not observed	7.01[d]
5	120	4.8	700	12	4.65
16	200	3.4	500	10	0.13
17	200	6.9	1000	10[c]	3.92
18	155	6.9	1000	9	4.52
19	98	6.9	1000	10	3.44
20	266	6.9	1000	Not observed	0.09[d]
21	177	4.8	700	10	1.71
22	177	3.4	500	14	0.73
23	44	6.9	1000	4	0.50
25	225	6.9	1000	Not observed	1.45[d]
27	155	5.5	800	8	3.99
28	155	3.4	500	13	5.33
				Av. = 10.2	
			In Carbon Monoxide		
37	200	2.1	300	22	6.28
38	200	1.1	160	28	1.76
39	220	1.2	170	28	1.71
40	242	1.2	170	33	8.29
				Av. = 27.8	

[a] Gas velocity above which $\dot{r}$ is independent of flow rate.

[b] At 20°C and 0.101 MPa (1 atm).

[c] Questionable.

[d] For a gas velocity = V_c (av.).

Temperature Effects

For the mixed gases a bell-shaped curve is obtained when $\dot{r}$ is plotted against temperature (Fig. 5). This curve, which is slightly skewed to the right, shows that $\dot{r}$ increases with temperature to a maximum at 177°C, then decreases sharply above this temperature to a very low value at 266°C. A similar plot is obtained for carbon monoxide; however, $\dot{r}$ reaches the maximum at about 246°C and falls off more rapidly with temperature than in the mixed gases. The formation rate of iron carbonyl for each gas at a P_{CO} of 1.17 MPa (170 psi) are compared in Fig. 6 to illustrate the large effect of the gas composition.

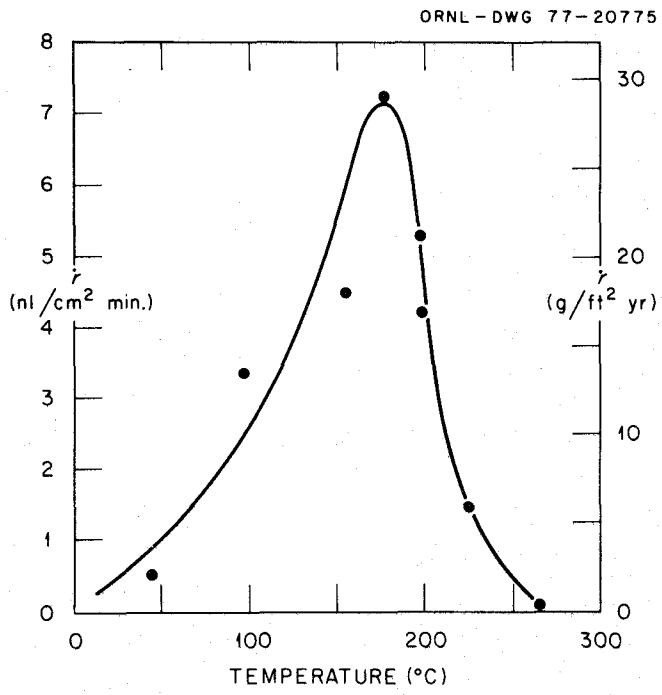

Fig. 5. Iron Carbonyl Formation is Governed by the Surface Reaction Rate Below 177°C and by Equilibrium Above This Temperature. The bell-shaped curve is a result of these competing processes. Data are for the mixed gases at 6.9 MPa flowing at 10.2 cm/min.

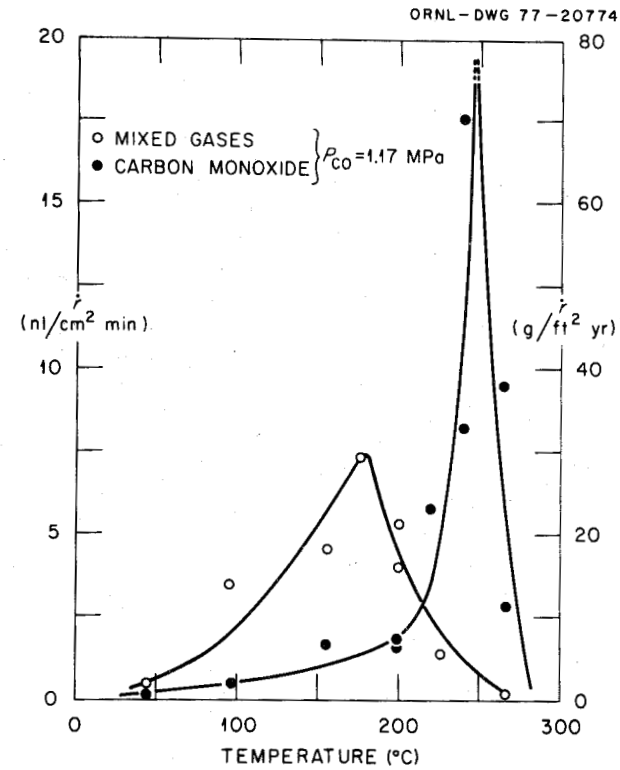

Fig. 6. Iron Carbonyl Formation Between 1/2% Mo Steel and Carbon Monoxide is Promoted or Retarded by H_2, CH_4, and/or CO_2, Depending on the Reaction Temperature. Comparison is for P_{CO} = 1.17 MPa (170 psi).

Pressure Effects

The dependence of $\dot{r}$ on the pressure of the mixed gases was determined from several separate runs (3, 4, 16, 17, 21, and 22 in Table 2), and the results are plotted in Fig. 7. The value of $\dot{r}$ is proportional to $P^{3.8}$ at 177°C and to $P^{5.0}$ at 200°C. In CO, $\dot{r}$ varied as $P_{CO}^{2.0}$ at or below 200°C and varied as $P_{CO}^{2.3}$ at 240°C (Fig. 8).

Effect of Test Gases on 1/2% Mo Steel

After the tests described above were completed, the steel pipes still had an adherent coating of Na_2SiO_3 on the external surfaces; however, the internal surfaces were covered with a black loose deposit assumed to be carbon. Analyses of turnings 0.51 mm thick from the inside surface of the pipes showed that the original carbon content of 0.05 wt % had increased to 0.30 wt % after testing in the gases.

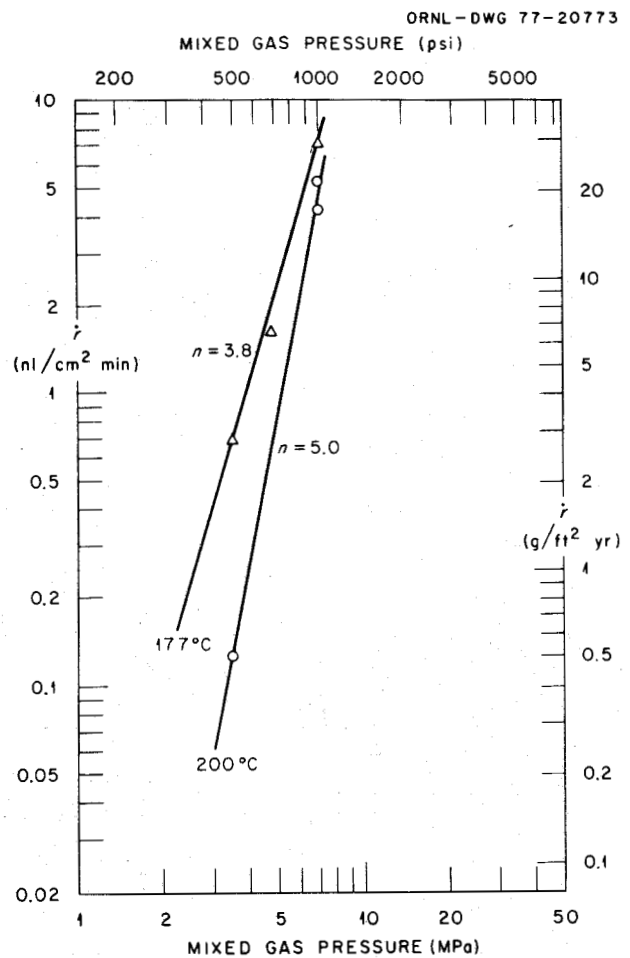

Fig. 7. The Formation Rate, $\dot{r}$, of Iron Carbonyl Between 1/2% Mo Steel and Mixed Gases Depends on the Pressure: $\dot{r} \propto P^n$. At 177°C, n = 3.8, and it increases to n = 5.0 at 200°C.

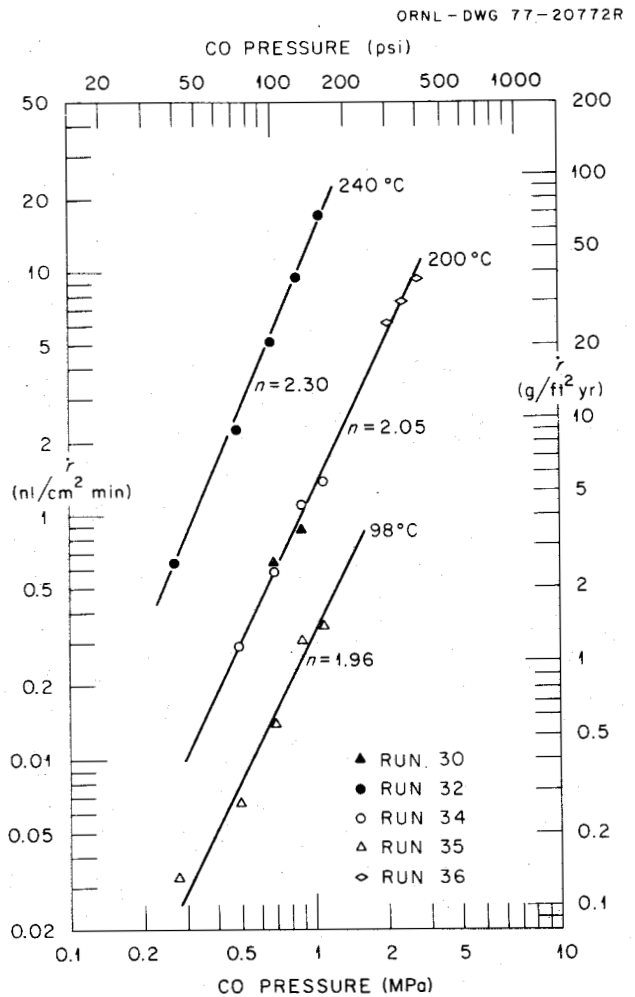

Fig. 8. The Formation Rate of Iron Carbonyl Between 1/2% Mo Steel and Carbon Monoxide Depends on the Pressure: $\dot{r} \propto P^n$, where $n \approx 2$ But Increases Slightly with Temperature.

Carbonyl Formation from Type 316 Stainless Steel

The reactions between type 316 stainless steel and the test gases were studied to determine whether the autoclave system was itself a source of carbonyls. No iron carbonyl was detected with either the mixed gases or carbon monoxide at temperatures to 300°C; however, at 200°C nickel carbonyl was measured in the effluent gases at concentrations just above the detection limit as shown in Fig. 9. The formation rate of nickel carbonyl between type 316 stainless steel and the mixed gases at 6.9 MPa is about 10 pl/cm^2 min (0.04 g/ft^2 year) at 200°C and decreases to about 7 pl/cm^2 min at 155°C.

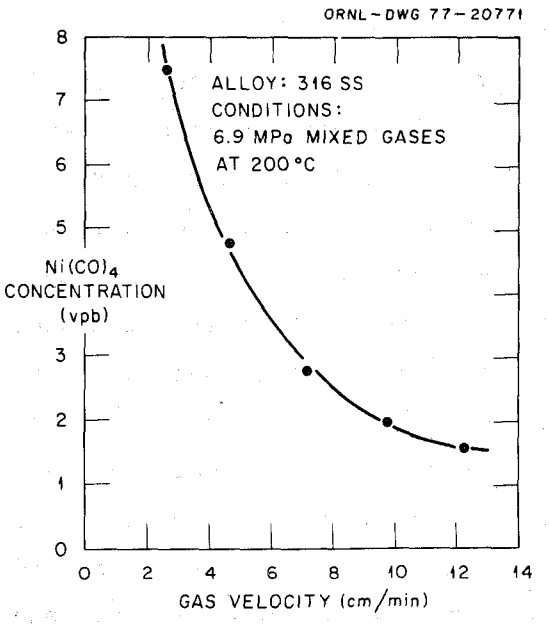

Fig. 9. Nickel Carbonyl Near the Detection Limit of the AAS Forms Between Type 316 Stainless Steel Autoclave and 6.9 MPa Mixed Gases. No iron carbonyl forms at 200°C.

DISCUSSION

The present results confirm that the formation rate, $\dot{r}$, of iron carbonyl between steels are carbon monoxide depends strongly on the gas flow rate, pressure, temperature, and steel composition; however,

this study further shows that the specific effects of these variables are significantly altered by the gases associated with the carbon monoxide, as discussed below.

Two distinct responses of $\dot{r}$ to the gas velocity are observed, depending on the temperature. At the lower temperatures $\dot{r}$ increases to a limiting value (Fig. 3), then becomes independent of the gas velocity. This suggests that $\dot{r}$ is diffusion limited up to a critical velocity, then becomes limited by a surface reaction. These critical velocities, V_c, in the mixed gases and in carbon monoxide were on the average 10.2 and 27.9 cm/min (Table 2), respectively, and were evident only in those tests run at the lower temperatures. That these velocities are in the same ratios as the molecular weights of the test gases (i.e., 11.9 and 28.0 g/mol) suggests that V_c is determined by the interdiffusion coefficients of carbon monoxide or the iron carbonyl in each gas. At the higher temperatures $\dot{r}$ increases continuously with the gas velocity and exhibits no tendency to stabilize at a fixed formation rate (Fig. 4). This characteristic appears to be associated with the carbonyl reaction reaching equilibrium, as discussed in the following text.

The increase in $\dot{r}$ with temperature is attributed to an increase in the rate of carbonyl reaction, and the sharp decrease in $\dot{r}$ with temperature at the higher temperature suggests that the reaction is approaching equilibrium. The competing processes result in the curves shown in Fig. 6. In Fig. 10, logarithms of iron carbonyl pressures attained in our tests with the 1/2% Mo steel in carbon monoxide at 1.17 MPa are plotted against $1/T$ and are compared with the equilibrium iron carbonyl pressures calculated from published[8—10] equilibrium constants for the reaction of pure iron with carbon monoxide. At the higher temperatures our data give $P_{Fe(CO)_5}$ values one to three orders of magnitude greater than the values based on published equilibrium data; however, the temperature dependence is almost the same as that predicted by Syrkin[8] or Brief.[9] The falloff of our iron carbonyl pressures from the log $P_{Fe(CO)_5}$ versus $1/T$ relationship at the lower temperatures suggests that the pressures are limited by the surface reaction rate. The equilibrium constant for the formation of iron carbonyl between

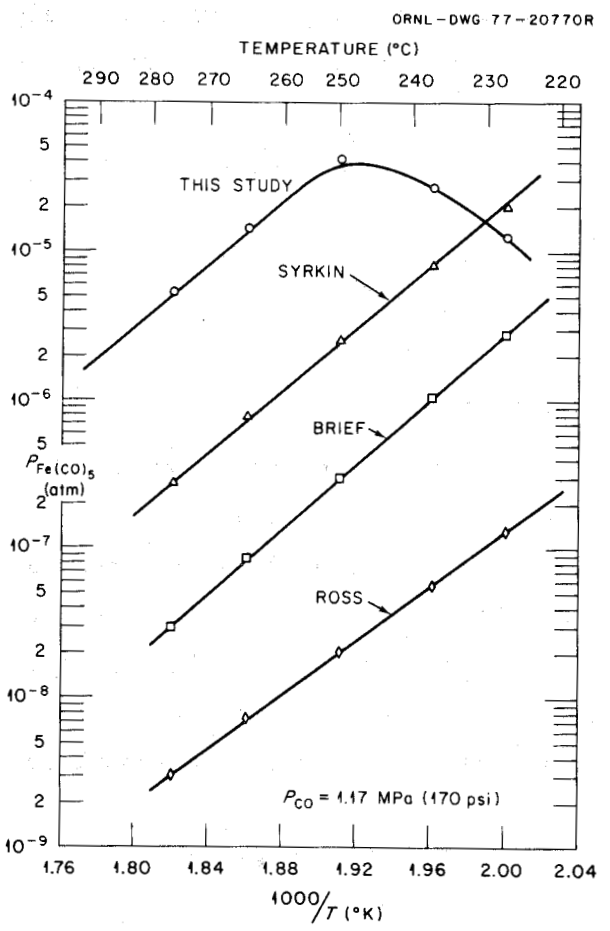

Fig. 10. In Equilibrium with 1.17 MPa Carbon Monoxide, $P_{Fe(CO)_5}$ is One to Three Orders of Magnitude Greater Than Published Data. Falloff from log $P_{Fe(CO)_5}$ versus $1/T$ relationship below about 250°C is due to nonequilibrium conditions. 1 atm = 0.10 MPa.

the 1/2% Mo steel and carbon monoxide above 245°C, based on our test data and assuming that the reaction is $Fe + 5CO \rightleftharpoons Fe(CO)_5$, is calculated to be

$$\log K = 9681/T - 28.188 \ , \qquad (1)$$

in terms of pressures expressed in atmospheres. Similar calculations for iron carbonyl formation between the steel and the carbon monoxide in the mixed gases above about 177°C resulted in an expression significantly different from Eq. (1) even in terms of its temperature dependence. This suggests that the carbonyl formation reaction in the mixed gases involves a different chemical sequence than in pure carbon monoxide.

Figures 7 and 8 show that $\dot{r}$ depends very strongly on the gas pressure and can be expressed by an equation of the form

$$\dot{r} = kP^n \ , \tag{2}$$

where

$\dot{r}$ = formation rate of $Fe(CO)_5$,

k = constant, and

P = partial pressure of CO.

Our results for tests in carbon monoxide show that n is not constant but increases with temperature between 98 and 240°C (i.e., from 1.96 to 2.30); however, these values are in general accord with a pressure dependency of approximately $P_{CO}^{2.0}$ as found by Stoffel.[6] As noted earlier, n also increases with temperature in the mixed gases, the pressure dependence being 3.8 at 177°C and 5.0 at 200°C.

If the equilibrium reaction for iron carbonyl formation is

$$Fe + 5CO \rightleftharpoons Fe(CO)_5 \ , \tag{3}$$

then the equilibrium constant is

$$K = P_{Fe(CO)_5}/P_{CO}{}^5 \ . \tag{4}$$

Thus, under conditions where the reaction rate to form iron carbonyl is sufficiently fast for the specimen surface to approach equilibrium with the gas before it leaves the reaction vessel, the limiting pressure of iron carbonyl, $[P_{Fe(CO)_5}]_{eq}$, is given by the product $K(P_{CO})^5$. Since

$$\dot{r} = \left[\frac{P_{Fe(CO)_5}}{P_{Total}}\right] \cdot \text{Flow Rate} \ , \tag{5}$$

then

$$\dot{r}_{max} = \left[\frac{KP_{CO}{}^5}{(1/X)P_{CO}}\right] \cdot \text{Flow Rate}, \tag{6}$$

or

$$\dot{r}_{max} = KX(P_{CO})^4 \cdot \text{Flow Rate}, \tag{7}$$

where

X = mol fraction of CO.

Under these limiting conditions, $\dot{r}$ should vary with the fourth power of the carbon monoxide pressure (at a given flow rate), or when $n = 4$, the iron carbonyl concentration is presumably approaching the equilibrium value.

On the other hand, the net reaction between iron and carbon monoxide must result in the formation of both iron carbonyl and free carbon as experimentally observed. Since Fe_3C is formed during the deposition of carbon,[11] a possible chemical sequence satisfying the observations might be as follows:

$$3Fe + 2CO \rightleftharpoons Fe_3C + CO_2 \ , \tag{8}$$

$$Fe_3C + 15CO \rightleftharpoons 3Fe(CO)_5 + C \ , \tag{9}$$

which when added give

$$3Fe + 17CO \rightleftharpoons 3Fe(CO)_5 + C + CO_2 \ . \tag{10}$$

Recalculation of the pressure dependence of iron carbonyl formation on P_{CO} in the manner described in Eqs. (5) through (7) and assuming that the reaction proceeds as in Eq. (10) gives $n = 4.7$ as the upper limit; that is, $\dot{r}$ should theoretically vary as the 4.7 power of the P_{CO} under conditions approaching equilibrium.

The reaction sequence given by Eqs. (8) and (9) is reasonably consistent with our test results for the mixed gases. In Fig. 6 we assumed that $\dot{r}$ at temperatures above the maxima is governed by thermodynamic equilibrium. This conclusion is corroborated by our prediction that $\dot{r} = kP_{CO}^{4.7}$, compared with a measured value of $\dot{r} = kP_{CO}^{5.0}$ in the mixed gases under conditions approaching equilibrium. Since our measurements

of the pressure dependence of $\dot{r}$ in CO were in the temperature range assumed to be governed by the surface reaction rate, values of $n < 4.7$ (e.g., $n = 2.0$ to 2.3) should be expected.

SUMMARY AND CONCLUSIONS

A 1/2% Mo steel was exposed to high-pressure carbon monoxide and to a gas mixture containing 17 CO—51 H_2—30 CH_4—2 CO_2 (vol %) to measure the rate of formation of iron carbonyl in steel piping leading to a methanation reactor. The variables affecting the formation rate, $\dot{r}$, were confirmed to be the gas velocity, temperature, and pressure. This study also shows that the presence of H_2, CH_4, and/or CO_2 in CO can significantly promote or retard the reaction of steel with CO, depending on the test conditions:

1. Rate $\dot{r}$ increases linearly with the gas velocity. Under equilibrium conditions, $\dot{r}$ is proportional to the gas velocity, but it reaches a limiting value above a critical velocity when the reaction is governed by the surface reaction rate.

2. Between 44 and 266°C, the formation rate, $\dot{r}$, of iron carbonyl increases with temperature to a sharp maximum at 245°C in 100% CO. The maximum occurs at 177°C when the CO is mixed with H_2, CH_4, and CO_2. Extrapolation of the rates to higher temperatures indicates that no iron carbonyl should form above 270°C for the mixed gases or above 285°C in carbon monoxide. The data further suggest that $\dot{r}$ is governed by the reaction rate up to the temperature of the maximum formation rate but that thermodynamic equilibrium is achieved above this temperature. The expression for the equilibrium constant for the reaction 1/2% Mo steel + CO $\rightleftharpoons$ $Fe(CO)_5$ was calculated to be

$$\log K = 9681/T - 28.188 \text{ in } 100\% \text{ CO},$$

when the pressures are expressed in atomospheres.

3. The equation $\dot{r} = kP_{CO}^{n}$ describes the pressure dependence of the formation of iron carbonyl on P_{CO}. In either gas, n increases moderately with temperature to a probable limiting value of 4.7 under

conditions approaching thermodynamic equilibrium. In contrast, when $\dot{r}$ is governed by the reaction rate, n is approximately 2.0.

ACKNOWLEDGMENTS

The authors thank W. C. Hawkins for running the experiments described in the manuscript. We are especially pleased with his accuracy and attention to the many details required to conduct these tests under safe and exacting conditions. The authors are also indebted to J. Brynestad for the design of the reaction rate apparatus and the development of the analytical techniques for determining iron and nickel carbonyls.

REFERENCES

1. A. J. Forney, Pittsburgh Energy Research Center, Private communication, 1975.
2. V. P. Sirohi, *Carbonyl Formation in Coal Gasification Plants*, C. F. Braun and Company, FE-2240-16 (December 1974).
3. J. Brynestad, *Iron and Nickel Carbonyl Formation in Steel Pipes and Its Prevention — Literature Survey*, ORNL/TM-5499 (September 1976).
4. R. L. Mond and A. E. Wallis, *J. Chem. Soc. (London)* 121: 29 (1922).
5. H. Pichler and H. Wallenda, *Brennst. Chem.* 21: 133 (1940). (Eng. Translation: The John Crerar Library Photoduplication Service, 35 W. 33rd Street, Chicago, Illinois.)
6. A. Stoffel, *Z. Anorg. Allg. Chem.* 84: 56 (1914).
7. R. S. Brief et al., *Arch. Environ. Health* 23: 373 (1971).
8. V. G. Syrkin, *Russ. J. Phys. Chem. (Eng. Transl.)* 48: 1718 (1974).
9. R. S. Brief, R. S. Ajemian, and R. G. Confer, *J. Am. Int. Hyg. Assoc.* 28: 21 (1967).
10. L. W. Ross, R. H. Haynie, and R. F. Hochman, *J. Chem. Eng. Data* 9: 339 (1964).
11. T. F. Berry, R. N. Ames, and R. B. Snow, *J. Am. Ceram. Soc.* 39: 308–18 (1956).

ORNL-5410
Distribution
Category UC-90d

INTERNAL DISTRIBUTION

1–2. Central Research Library
3. Document Reference Section
4–6. Laboratory Records Department
7. Laboratory Records, ORNL RC
8. ORNL Patent Office.
9. M. Bender
10. N. K. Bernander (Y-12)
11. H. D. Cochran, Jr.
12. K. V. Cook
13. K. E. Cowser
14. E. V. Davis
15. V. A. DeCarlo
16–20. J. H. DeVan
21. C. V. Dodd
22. W. P. Eatherly
23. D. P. Edmonds
24. D. E. Ferguson
25. L. M. Ferris
26. B. E. Foster
27. W. Fulkerson
28. J. W. Garber (Y-12)
29. T. G. Godfrey
30. G. M. Goodwin
31. R. J. Gray
32. W. L. Greenstreet
33. J. R. Hightower
34–36. M. R. Hill
37. R. S. Holcomb
38. J. M. Holmes
39. J. K. Huffstetler
40–44. H. Inouye
45. V. C. Jackson (Y-12)
46. G. R. Jasny (Y-12)
47. J. E. Jones, Jr.
48. R. T. King
49. W. J. Lackey
50. W. R. Laing
51. J. S. Lin
52. R. S. Livingston
53. P. L. Long (Y-12)
54. R. E. MacPherson
55. W. R. Martin (Y-12)
56. D. L. Mason (Y-12)
57. W. J. Mason
58. R. W. McClung
59. R. E. McDonald
60. L. E. McNeese
61. J. R. McWherter
62. H. J. Metz
63. C. S. Morgan
64. F. D. Mundt (K-25)
65. J. P. Nichols
66. L. C. Oakes
67. T. W. Pickel
68. H. Postma
69. C. R. Richmond
70. M. W. Rosenthal
71. T. H. Row
72. R. Salmon
73. G. Samuels
74. C. D. Scott
75. G. W. Scott
76. W. A. Simpson, Jr.
77. G. M. Slaughter
78. J. H. Smith
79. R. F. Smith (K-25)
80. S. D. Snyder
81. I. Spiewak
82. V. J. Tennery
83. H. E. Trammell
84. D. B. Trauger
85. G. D. Whitman
86. L. V. Wilson
87. C. S. Yust
88. L. Adler (consultant)
89. S. Alpert (consultant)
90. H. Beuther (consultant)
91. M. Semchyshen (consultant)
92. H. W. Sternberg (consultant)
93. C. Streed (consultant)

EXTERNAL DISTRIBUTION

94. Ames Laboratory, 205 Met. Dev. Bldg., Iowa State University, Ames, IA 50011

T. E. Scott

95–102. Argonne National Laboratory, 9700 South Cass Avenue, Argonne, IL 60439

O. K. Chopra
Steven Danyluk
W. A. Ellingson
K. Natesan
J. Y. Park
W. J. Shack
D. Stahl
R. Swaroop

103. Babcock & Wilcox Company, P.O. Box 1260, Lynchburg, VA 24505

E. M. Anderson

104–107. Battelle Columbus Laboratories, 505 King Avenue, Columbus, OH 43201

A. M. Hall
J. J. Mueller
J. R. Schorr
I. G. Wright

108. Battelle Pacific Northwest Laboratory, P.O. Box 999, Richland, WA 99352

J. J. Bates

109. CNG Energy Company, Four Gateway Center, Pittsburgh, PA 15222

David A. Damon

110. Cabot Corporation, Stellite Division, 1020 Park Avenue, Kokomo, IN 46901

R. B. Herchenroeder

111. Columbia Gas System Service Corporation, 1600 Dublin Road, Columbus, OH 43215

Jane Breitmeier

112. Combustion Engineering, Inc., 1000 Prospect Hill Road, Windsor, CT 06905

A. L. Plumley

EXTERNAL DISTRIBUTION (Continued)

113. Combustion Engineering Power Systems, 911 West Main Street, Chattanooga, TN 37402

E. C. Lewis

114–116. Electric Power Research Institute, 3412 Hillview Avenue, Palo Alto, CA 94304

C. F. Culler
R. I. Jaffee
I. Stringer

117. Exxon Research and Engineering Company, P.O. Box 51, Linden, NJ 07036

M. S. Nutkis

118. FluiDyne Engineering Corporation, P.O. Box Drawer 1465, Springfield, VA 22151

L. R. White

119. Foster-Wheeler Development Corporation, 12 Peach Tree Hill Road, Livingston, NJ 07039

I. M. Rehn

120–123. General Electric Company, 1 River Road, Schenectady, NY 12019

M. B. Cutrone
H. V. Doering
R. M. Goldhoff
R. L. McCarron

124. International Nickel Company, Sterling Forest, Suffern, NY 10901

E. P. Sadowski

125. Lockheed Palo Alto Research Laboratories, 3251 Hanover Street, Palo Alto, CA 94304

R. A. Perkins

126. Metals Properties Council, Inc., 1351 Butler Pike, Blue Bell, PA 19422

A. O. Schaefer

127. National Bureau of Standards, Washington, DC 20234

J. H. Smith

EXTERNAL DISTRIBUTION (Continued)

128. Pratt & Whitney Aircraft, Aircraft Road, Middletown, CT 06457

T. S. Pettit

129. Rensselaer Polytechnic Institute, Department of Materials Engineering, Troy, NY 12181

John B. Hudson

130. Sandia Laboratories, Livermore, CA 94550

R. Bradshaw

131—132. Solar Turbines International, 2200 Pacific Highway, P.O. Box 80966, San Diego, CA 92122

A. G. Metcalfe
M. E. Ward

133. Union Carbide Corporation, P.O. Box 8361, South Charleston, WV 25303

William McGoldrick

134. University of Notre Dame, Box E, Met. Eng. and Materials Science, Notre Dame, IN 46556

N. F. Fiore

135. U.S. Bureau of Mines, P.O. Box 70, Albany, OR 97321

F. W. Wood

136—140. Westinghouse Electric Corporation, 1310 Beulah, Pittsburgh, PA 15235

R. J. Bratton
T. J. Harvey
J. D. Landes
D. Moon
T. Vojnovich

141—143. DOE Office of Fossil Energy, 20 Massachusetts Avenue Northwest, Washington, DC 20545

W. T. Bakker
John Fairbanks
H. E. Frankel

144—145. DOE OAK RIDGE OPERATIONS OFFICE, P.O. Box E, Oak Ridge, TN 37830

Research and Technical Support Division

EXTERNAL DISTRIBUTION (Continued)

146–456. DOE TECHNICAL INFORMATION CENTER, Office of Information Services, P.O. Box 62, Oak Ridge, TN 37830

For distribution as shown in TID-4500 Distribution Category, UC-90d (Coal Conversion and Utilization — Liquefaction).